ACTIVE MAGNETIC BEARINGS FOR THE IDENTIFICATION OF DYNAMIC CHARACTERISTICS OF FLUID BEARINGS—CALIBRATION RESULTS

E. Knopf,[1] R. Nordmann[2]

ABSTRACT

Active magnetic bearings, a typical mechatronic product, are getting more and more common in turbomachinery. Besides their function of an oil-, contact- and frictionless levitation of the rotor (Schweitzer et al, 1993), they are best suited to be used as a measurement instrument to extract more information from the system under observation. The aim of the presented DFG-project (German Research Council) is to use active magnetic bearings as an accurate measurement and excitation device for the identification of linear and nonlinear dynamic characteristics of flow medium lubricated journal bearings. This type of bearing is often used in centrifugal pumps as an alternative to conventional oil-lubricated bearings. Contrary to oil lubrication, the flow medium often has a very small viscosity, which leads to a turbulent lubricating film. This turbulence causes essential changes in the dynamic characteristics of the bearings. The influence of journal bearings on the dynamics of the pump system is caused by Fluid-Structure-Interactions (FSI) (Gasch, Pfützner, 1975, Matros et al, 1994). FSI occur in the presence of relative motion between rotating and stationary part of the bearing. In the presented project the active magnetic bearings are on the one hand used to levitate the rotor and to operate as actuators to generate the relative motion. On the other hand, the magnetic bearings are used to measure the enforced displacements and the resulting forces induced in the rotating structure in a very accurate way.

EXPERIMENTAL METHOD

Figure 1 shows the basic design of the testrig. In normal operation the rotor is supported by two magnetic bearings. The journal bearing is located between the two AMBs. The rotor is connected to a synchronous motor via a flexible coupling (low stiffness in radial direction, high stiffness in torsional direction). The whole unit is mounted on a rigid foundation and vibrational isolated to the ground. For the evaluation of linear journal bearing dynamics, the rotor is set to defined offset positions. These eccentric positions are causing static fluid forces in the journal bearing due to hydrodynamic effects. Subsequently an additional defined displacement excitation around the operating point is enforced. The journal bearing reacts with dynamic forces caused by Fluid-Structure-Interactions which can be described by stiffness-, damping- and inertia-coefficients (linear dynamics). In the case of nonlinear investigations, the rotor will

[1]Department of Mechatronics, Techn. University of Darmstadt, Petersenstr. 30, 64289, Darmstadt, Germany, e-mail: knopf@mesym.tu-darmstadt.de.
[2]Department of Mechatronics, Techn. University of Darmstadt, Petersenstr. 30, 64289, Darmstadt, Germany, e-mail: nordmann@mesym.tu-darmstadt.de.

be set to large orbits in the journal bearing (up to 90% of journal bearing clearance). The description of the dynamic behavior is carried out by force-displacement relationships.

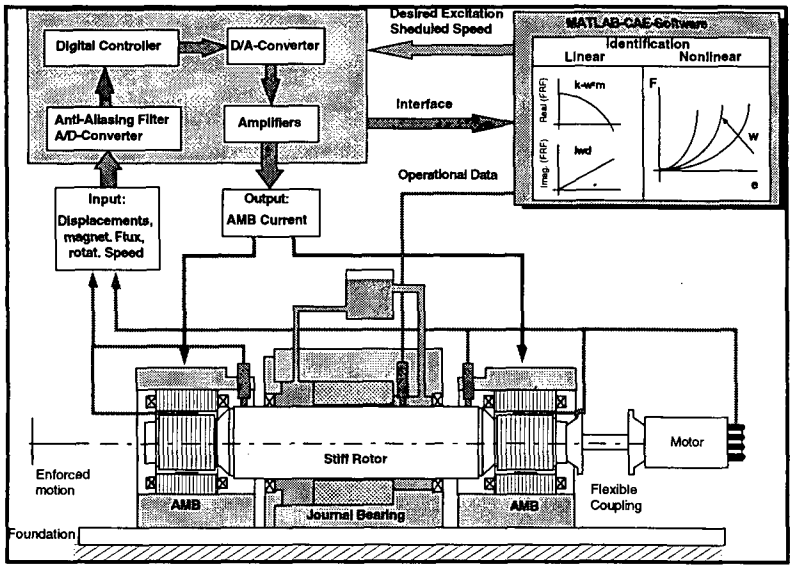

Figure 1: Scheme of experimental setup

The rotor has no elastic eigenfrequency within the operating range. Therefor the displacements and the forces that occur in the journal bearing can easily be computed with the help of the displacements and the forces measured in the magnetic bearings (only geometric transformations). The magnetic forces are computed on-line from the magnetic flux densities measured by the hallsensors.The hall sensors are located at each magnetic pole. The actual signal processing and data analysis is done using standard CAE- Software.

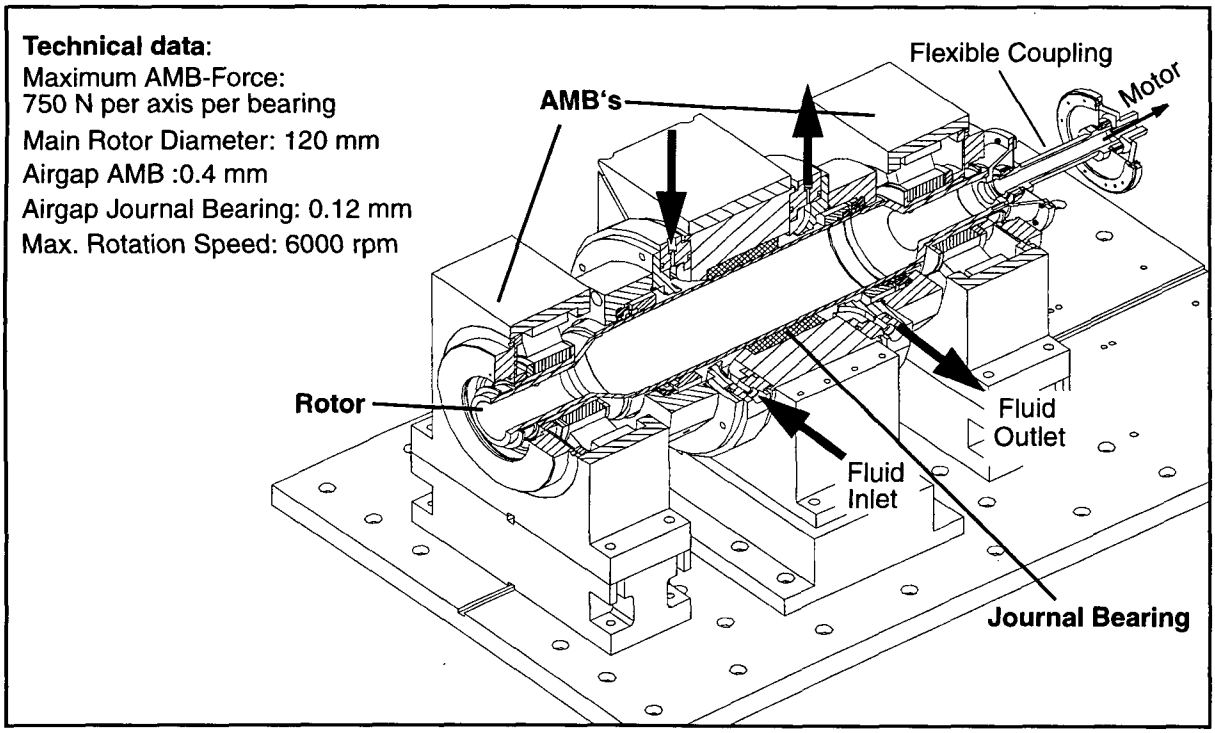

Figure 2: Designed testrig

The testrig is designed in a modular way. Figure 2 shows the realized testrig in the configuration with cylindrical journal bearing. The journal bearing is axially supplied with the lubricant and sealed up against atmosphere by two mechanical seals (low stiffness in radial direction). The rotor consists of a hollow shaft with two laminated radial bearing units shrink fitted to the shaft (1. elastic eigenfrequency:1079 Hz).

FORCE MEASUREMENT METHOD

The precision of the identification procedure depends on the precision of the force measurement. As the dynamic behavior of the journal bearing depends on the offset position (static eccentricity), the rotor consequently is operated in different offset positions and the applied AMB-forces vary in a wide range up to maximum AMB-forces. Hence the applied force measurement method must be valid for the whole range of magnetic forces and for all possible rotor positions. The most promising method to realize this is to use hall sensor elements in all magnetic poles, measuring the magnetic flux Φ at each pole (for a given area A and permeability μ_0, see Fig.3).

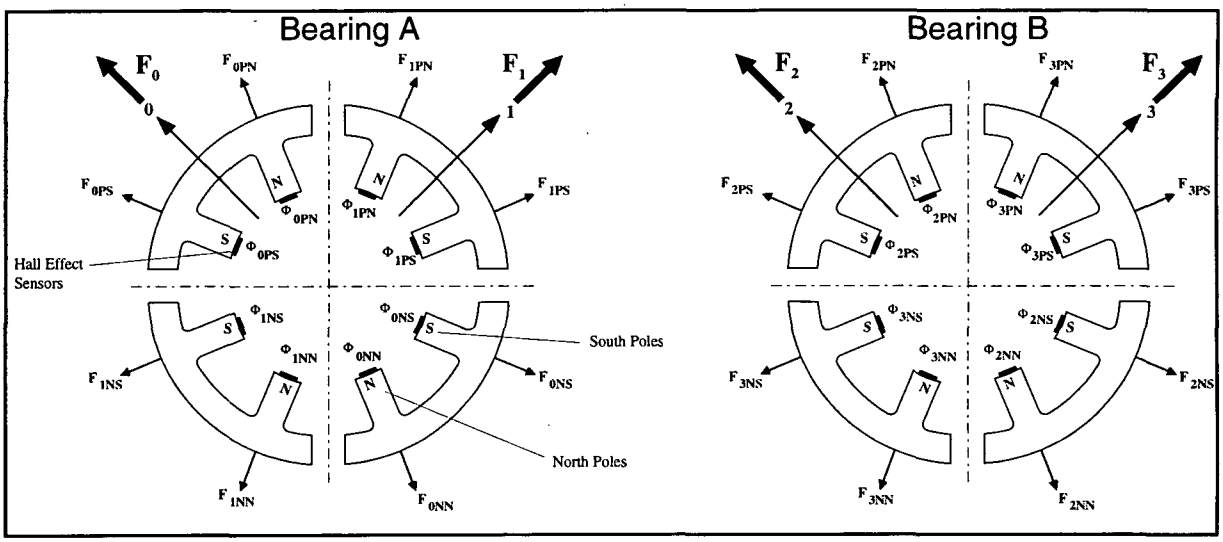

Figure 3: Force computation

The force at each pole is proportional to Φ^2. The resulting forces acting in the global directions 0...3 can be computed with (e.g. for bearing axis 0):

$$F_0 = \frac{1}{A \cdot \mu_0} \cdot \qquad (1)$$

$$[cos\pi/8 \cdot (\Phi_{0pN}^2 + \Phi_{0pS}^2 - \Phi_{0nN}^2 - \Phi_{0nS}^2) + sin\pi/8 \cdot (\Phi_{1pN}^2 - \Phi_{1pS}^2 - \Phi_{1nN}^2 + \Phi_{1nS}^2)$$

Equation (1) is also satisfied for saturation and hysteresis effects. The prefactors can be derived from calculation or for higher accuracy from calibration.

Advantages of direct force measurement via hall effect sensors:
- -due to direct measurement of magnetic fluxes at all poles, no further assumption or approximations have to be made
- -nonlinear effects like amplifier saturation do not influence the measurement
- - the force is measured directly at the interface to the rotating structure

Disadvantages:
- - increase of air gap leads to lower maximum forces (for unchanged ampere windings)
- - higher hardware effort due to additional sensor elements

CALIBRATION OF THE MAGNETIC FORCES

The calibration of the magnetic forces is done using known external static forces (Förch et al. 1994). The external forces are measured with a load cell connected momentum free to the rotor. With the known geometry, the applied forces are transformed into the bearing planes and can be compared with the reaction forces generated in the magnetic bearings which leads to force errors parallel and orthogonal to the external force direction.

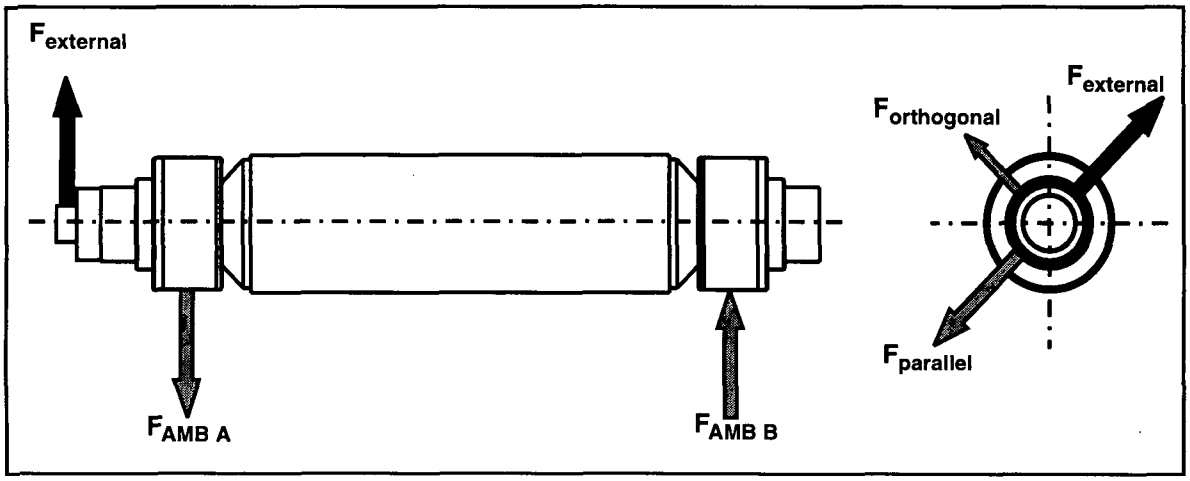

Figure 4: Scheme for static force calibration

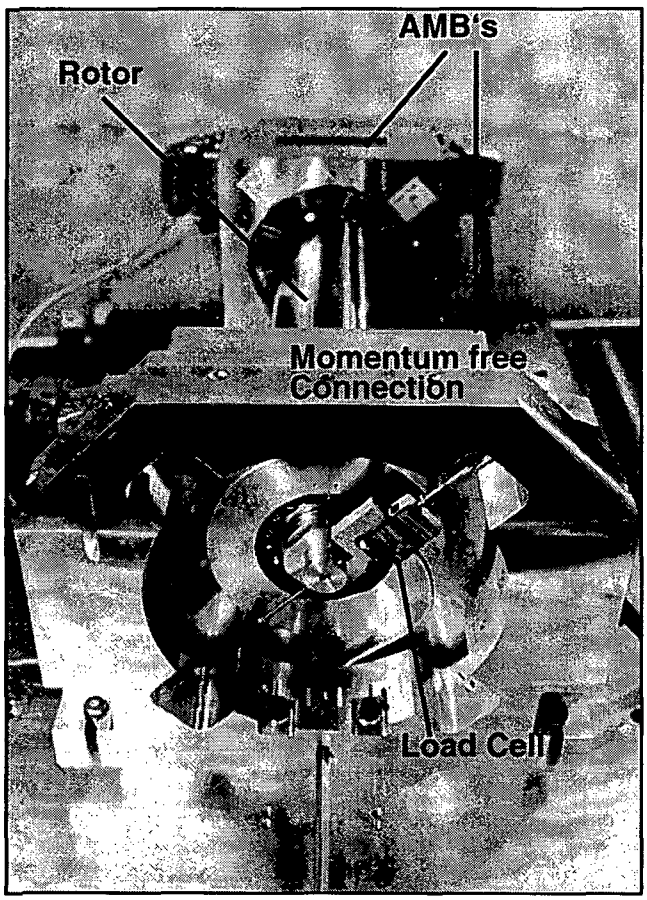

Figure 5: Setup for static calibration procedure

The position of the load cell can be changed to measure different bearing axes. The static force calibration was performed with external forces parallel to the magnetic bearing axes, for horizontal and vertical force input, for different force ranges up to 700 N and for different static offset positions of the rotor up to 0.3 mm (75% of backup bearing clearance). The hysteresis cycles were measured in directions parallel and orthogonal to the force input directions.

Results:

With the rotor floating in the nominal position the resulting force errors are presented in Fig. 6. The averaged force error parallel to the bearing axes is about 5 N (= 0.7% of the external force). The maximum static force errors are below 1% of the external force. It can be seen, that in general the force error decreases for an input in horizontal or vertical direction. This can be explained by a partly compensation of hysteresis curves of the individual bearing axes.

TABLE I: STATIC FORCE ERRORS

Rotor at nominal position	Average force error	Worst case	Cross coupling error (Worst case)	Hysteresis error (Worst case)
Force Input in direction of AMB axes **Range 700 N**	5 N ⇒ 0.7%	6.8 N ⇒ 0.97%	4 N ⇒ 0.6%	3 N ⇒ 0.4%
Horizontal/Vertical Force Input **Range 700 N**	**3.5 N** ⇒ 0.5%	**5 N** ⇒ 0.7%	**6 N** ⇒ 0.86%	**2 N** ⇒ 0.3%

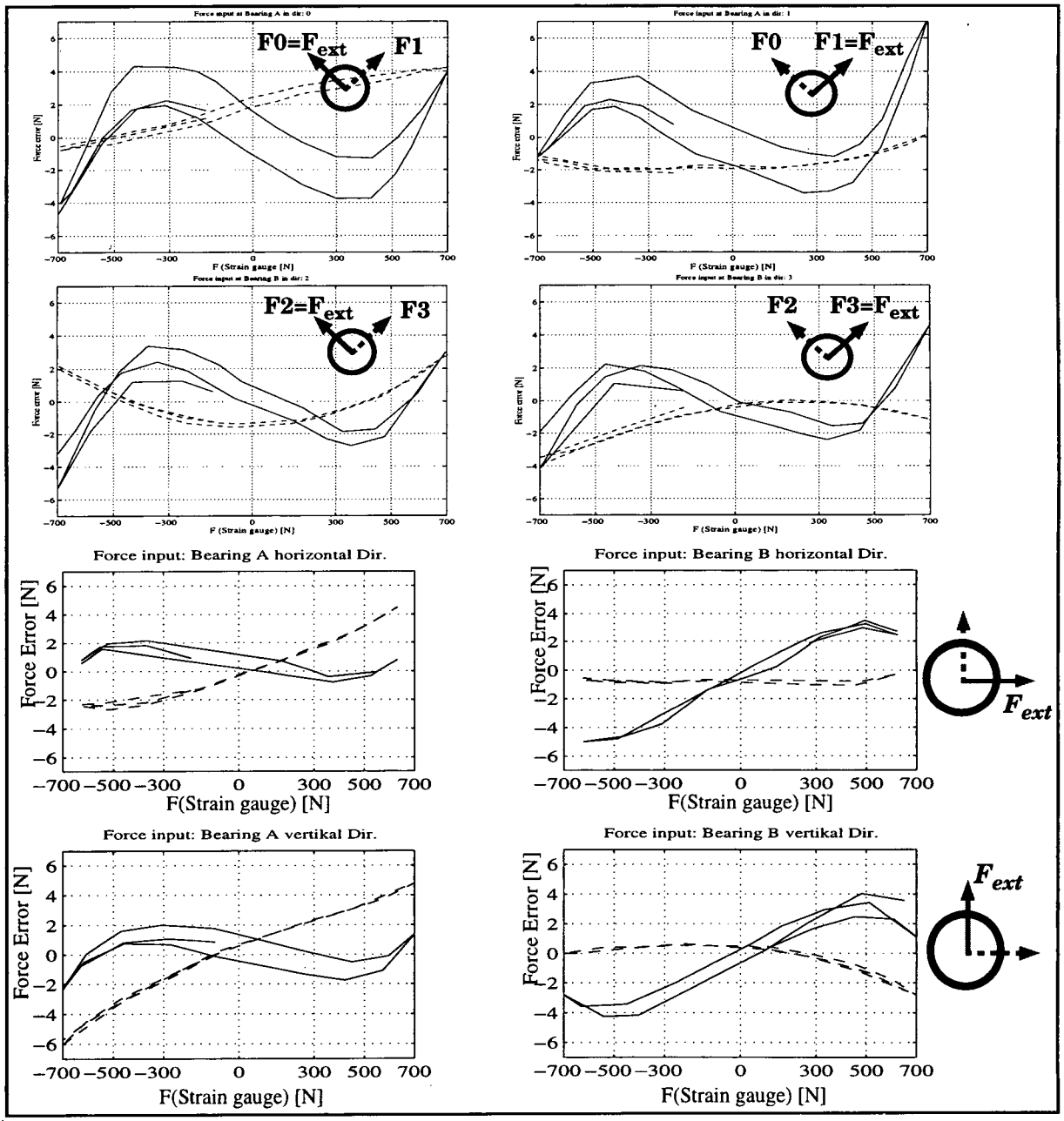

Figure 6: Magnetic bearing force errors for different directions of external force input. Force range: 700 N (solid lines: Force error parallel to external force; dashed lines: Force error orthogonal to the external force)

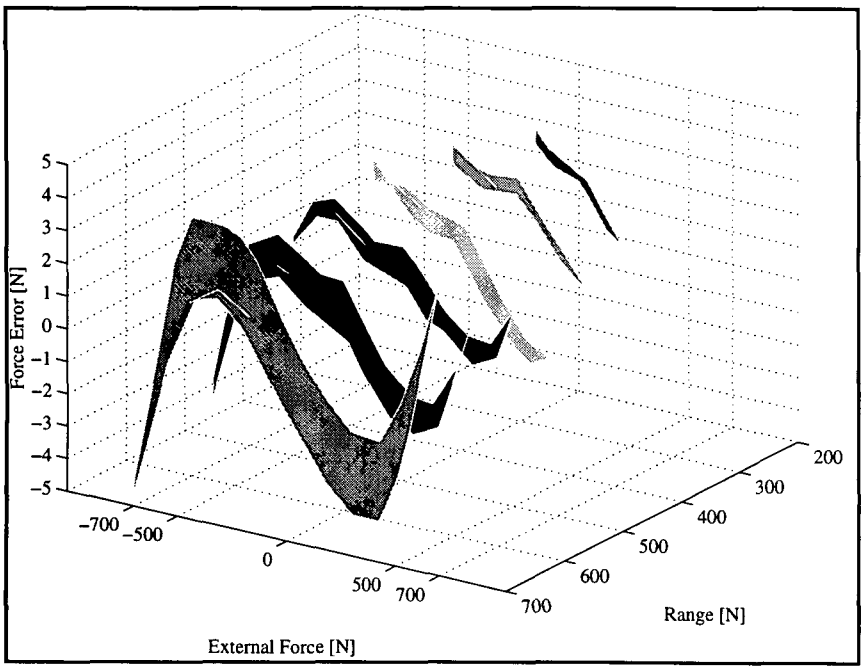

Figure 7: Force errors for different ranges of external force

Figure 7 shows hysteresis cycles for different ranges of external forces. It is obvious, that the force error for smaller ranges could be improved by tuning the gain factors. But as mentioned before, the main attention lies on the accurate measurement of large AMB forces, so the gain factors were chosen to minimize the error at force ranges of 700 N. Figure 8 shows some results from static calibration procedure performed at different offset positions of the rotor. The overall force error increases with the static eccentricity of the rotor. It is evident, that a main part of the overall force error is caused by an offset error which has no influence on dynamic measurements.

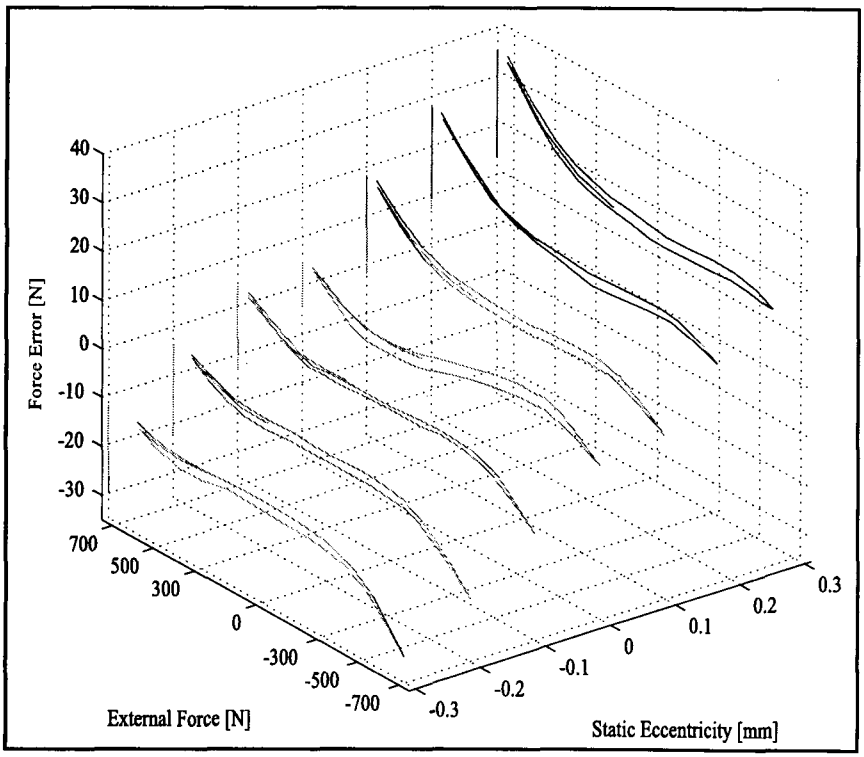

Figure 8: Magnetic bearing force errors for different static offset positions of the rotor

This offset error shows a quite linear dependence on the static position of the rotor. Figure 9 shows the offset error while moving the rotor stepwise on an orbit of 0.1 mm. The offset is symmetric around the circumference of the bearing. We assume that this error is caused by a change of the stray flux distribution with the offset positions, which is not measured by the hallsensors. Regarding the hysteresis cycles themselves, they get more and more unsymmetrical due to uneven airgaps and consequently uneven saturation states of two opposite pole pairs.

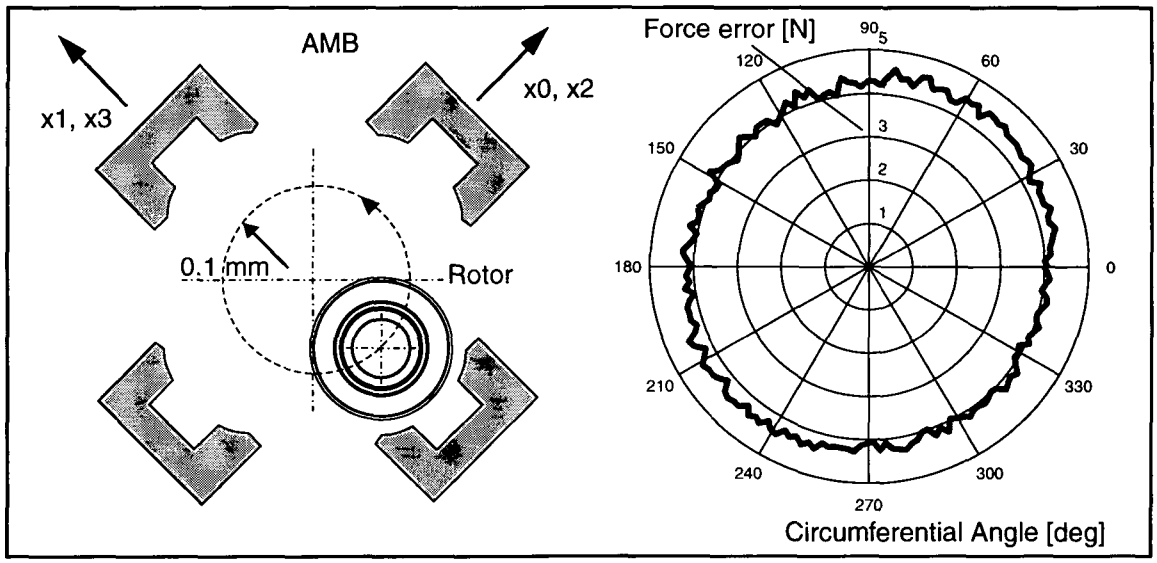

Figure 9: Magnetic bearing force error for a step-by-step orbital movement of the rotor

TABLE II: STATIC FORCE ERRORS FOR DIFFERENT OFFSET POSITIONS OF THE ROTOR

Rotor at eccentrical positions Force Range 700 N	Overall force error	Force error without offset error	Cross coupling error (Worst case)	Hysteresis error (Worst Case)
Static offset 0.1 mm	15 N ⇒ 2.1 %	10 N ⇒ 1.4 %	5 N ⇒ 0.7%	2.5 N ⇒ 0.4 %
Static offset 0.3 mm	35 N ⇒ 5 %	20 N ⇒ 2.8 %	6 N ⇒ 0.9%	3 N ⇒ 0.4 %

VERIFICATION OF THE FORCE MEASUREMENT METHOD

The verification of the force measurement method is realized with the identification of well known physical properties, such as the mass of the rotor.

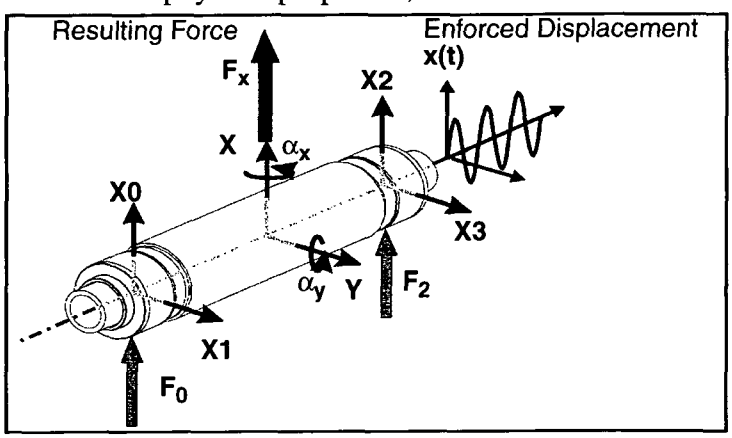

Figure 10: Degrees of freedom of the rotor

The method is identical to the later used method for identification of journal bearing characteristics. The rotor is sinusoidal excited via defined displacements at discrete frequencies and the forces which are necessary to generate this motion are measured. Thus the forces are measured directly in the airgap, only the transfer functions of the plant (rotor) are measured. The rotor is dynamically stiff in the applied frequency range, which means that it can be considered as a lumped mass and therefore only inertia effects occur. The parameter identification of the inverse frequency response functions leads to the identification of the mass matrix

of the free rotor. Figure 11 shows inverse frequency response functions measured at rotational speed of 5000 rpm with a displacement amplitude of 0.005 mm in one plane. The response is measured in the four DOFs of the magnetic bearings and transformed to the center of gravity (decoupling of the equation of motion). An excitation e.g in the x-direction corresponds to the identification of one column of the mass matrix (real part of the transfer function, imaginary part of the transfer function should be zero).

$$\begin{bmatrix} x \\ y \\ \alpha_x \\ \alpha_y \end{bmatrix} = [T] \cdot \begin{bmatrix} x_0 \\ x_1 \\ x_2 \\ x_3 \end{bmatrix} \text{ and } \begin{bmatrix} F_x \\ F_y \\ M_x \\ M_y \end{bmatrix} = [T] \cdot \begin{bmatrix} F_0 \\ F_1 \\ F_2 \\ F_3 \end{bmatrix} \tag{2}$$

$$\begin{bmatrix} \hat{F}_x \\ \hat{F}_y \\ \hat{M}_x \\ \hat{M}_y \end{bmatrix} = -\omega^2 \cdot \begin{bmatrix} m & 0 & 0 & 0 \\ 0 & m & 0 & 0 \\ 0 & 0 & \Theta_x & 0 \\ 0 & 0 & 0 & \Theta_y \end{bmatrix} \cdot \begin{bmatrix} \hat{x} \\ \hat{y} \\ \hat{\alpha}_x \\ \hat{\alpha}_y \end{bmatrix} \tag{3}$$

After curve-fitting, the overall identification error of the rotor mass (m=16.75 kg) at standstill is below 0.3% for displacement amplitudes of 0.01 mm, respectively below 0.8% for displacement amplitudes of 0.005 mm. The identification error gets slightly bigger for the rotating rotor but is below 2% (0.01 mm) resp. about 3% (0.005 mm). For an eccentric position of almost journal bearing clearance (0.1 mm) the error increases to 3% (0.01 mm) resp. 4% (0.005 mm). Figure 12 gives a more detailed description of the identification error at discrete excitation frequencies. It can be seen, that the identification error is below 1% (0.01 mm), respectively below 1.7% (0.005 mm) for excitation frequencies greater than 50 Hz. The error increases strongly for lower frequencies which is mainly caused by very small forces (see Figure 11). It can be assumed that the identification error decreases for lower frequencies when a substantial force is present such as in the case of the journal bearing being mounted.

TABLE III: MASS IDENTIFICATION ERRORS

		Mass Identification Error
Rotor at centered position	**Rotor at standstill** Displacement Amplitude 0.01 mm	**0.3%**
	Rotor at standstill Displacement Amplitude 0.005 mm	**0.8%**
	Rotor at 5000 rpm Displacement Amplitude 0.01 mm	**2.0%**
	Rotor at 5000 rpm Displacement Amplitude 0.005 mm	**2.5%**
stat. offset 0.1 mm	**Rotor at 5000 rpm** Displacement Amplitude 0.01 mm	**3.0%**
	Rotor at 5000 rpm Displacement Amplitude 0.005 mm	**4.0%**

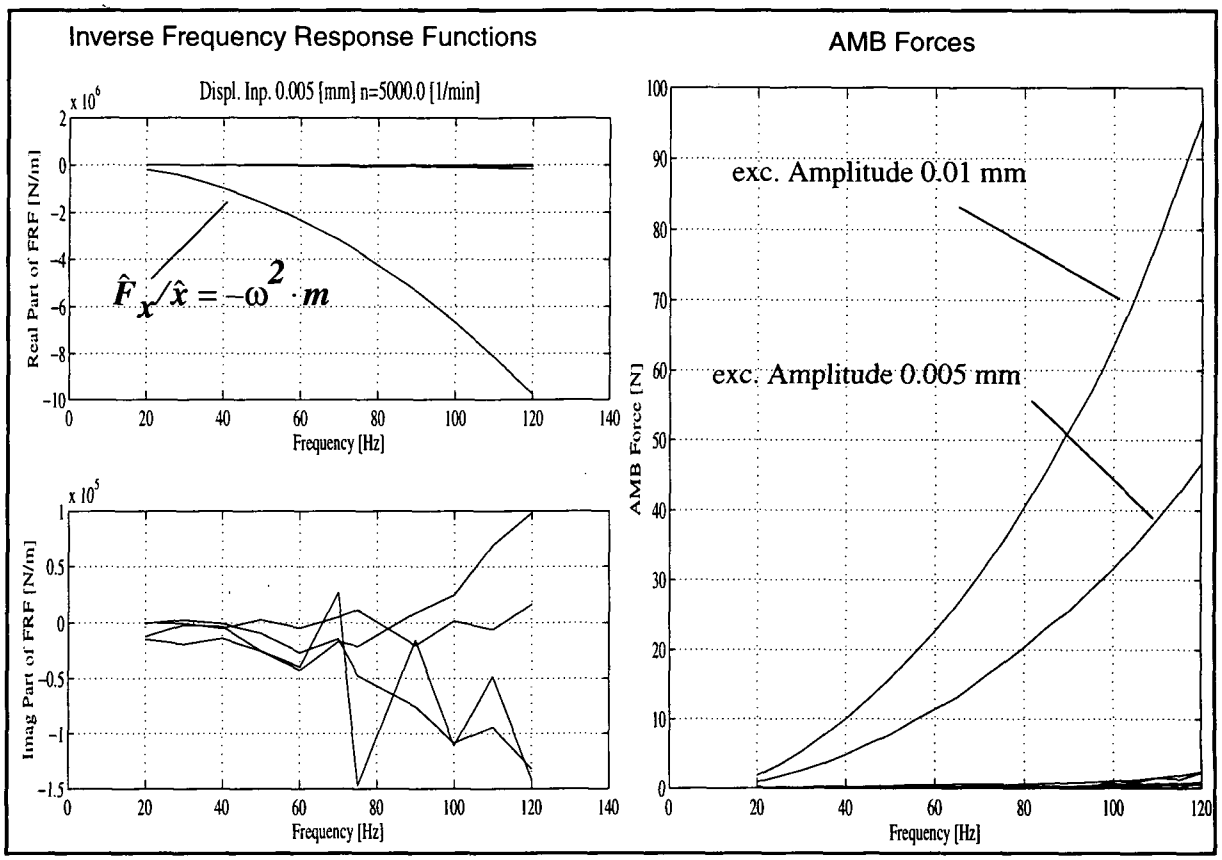

Figure 11: Inverse frequency response function of the rotor (exc. Amplitude 0.005 mm; rot. Speed 5000 rpm) and measured AMB forces for given displacement amplitudes

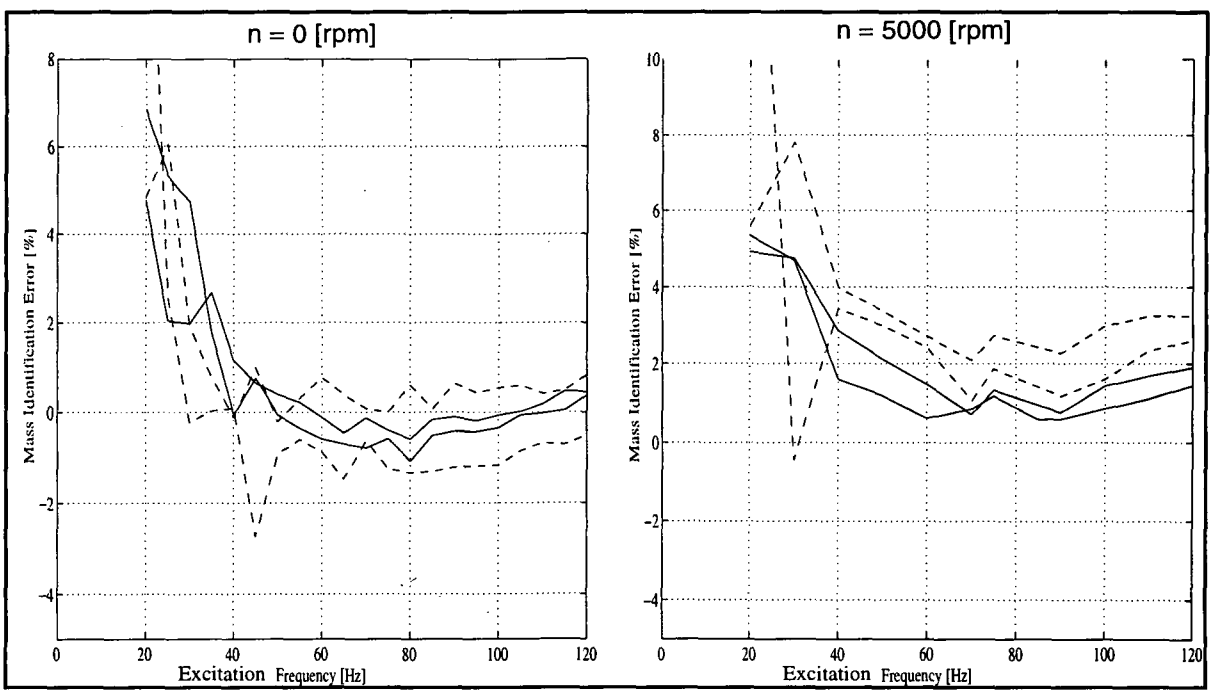

Figure 12: Relative mass identification errors measured at standstill and for a rot. speed of 5000 rpm (solid lines: exc. Ampl. 0.01 mm; dashed lines: exc. Ampl. 0.005 mm)

CONCLUSION AND OUTLOOK

A novel designed testrig for the identification of the dynamic behavior of turbulent journal bearings using active magnetic bearings has been presented. The magnetic bearings are used as actuators and as a device for the accurate measurement of generated forces. The accuracy of the implemented force measurement has been confirmed during a calibration and verification procedure. The force measurement method by using hall effect sensors in all magnetic poles has essential advantages compared to conventional methods. The method is valid for the whole range of possible AMB forces.

ACKNOWLEDGMENT

The presented paper is a result from research work sponsored by the German Research Council (DFG) under contract number N0 136/16-2.

REFERENCES

P.Förch, A. Reister, C. Gähler, R. Nordmann: Modal Analysis of Rotating Structure, Vibrations in Rotating Machinery, SIRM, 1994

C. Gähler, P. Förch: A Precise Magnetic Bearing Exciter for Rotordynamic Experiments, 4th International Symposium on Magnetic Bearings, Zurich, Switzerland, 1994

R. Gasch, H. Pfützner: Rotor Dynamics, Springer Verlag, 1975

M. Matros, T. Neumer, R. Nordmann: Identification of Rotordynamic Coefficients of Centrifugal Pump Components Using Active Magnetic Bearings.
Preprint of the ISROMAC-5,1994.

R. Nordmann: Identification Techniques in Rotordynamics, Symposium on Diagnostics of Rotating Machines in Power Plants, Udine, Italy, 1993

G. Schweitzer, H. Bleuler, A. Traxler: Active Magnetic Bearings.
Verlag der Fachvereine, Zurich, Switzerland, 1993